Regular Article

INORGANIC CHEMISTRY RESEARCH
Published by the
Iranian Chemical Society
www.inorgchemres.org
info@inorgchemres.org

Inorg. Chem. Res., *Vol. 1, No. 1, 9-20, June 2016*
DOI: 10.22036/icr.2016.33228

Electrochemistry, Thermalanalysis, and Theoretical Study of Vanadyl Schiff Base Complexes

A.H. Kianfar[a,*], H. Mohamadi Malek Abadi[b], R. Hashemi Fath[b] and M. Roushani[c]

[a]*Department of Chemistry, Isfahan University of Technology, Isfahan, Iran,* 84156-83111
[b]*Department of Chemistry, Yasouj University, Yasouj, Iran*
[c]*Department of Chemistry, Ilam University, Ilam, Iran*

(Received 2 June 2014, Accepted 13 May 2016)

The VO(IV) complexes of tridentate ONO Schiff base ligands derived from 2-aminobenzoicacid and salicylaldehyde derivatives were synthesized and characterized by IR, UV-Vis and elemental analysis. Electrochemical properties of the vanadyl complexes were investigated by cyclic voltammetry. A good linear correlation was observed between the oxidation potentials and the electron-withdrawing character of the substituents on the Schiff bases, showed the following trend: MeO < H < Br < NO_2. The thermogravimetry (TG) and differential thermoanalysis (DTA) of the synthesized complexes were carried out in the range of 20-700 °C. All of the complexes decomposed in three steps. The thermal decomposition pathways were closely related to the nature of the Schiff base ligands and preceded *via* first-order kinetics. The structures of compounds were determined by *ab initio* calculations. The optimized molecular geometry was calculated at the B3LYP/6-31G(d) level. The results suggested that, in the complexes, V(IV) ion was in square-pyramid or TBP (trigonal bipyramidal) NO_4 coordination geometry. Also the bond lengths and angles were studied and compared.

Keywords: Vanadyl complexes, Tridentate schiff base ligands, Schiff base complexes, Thermogravimetry, Electrochemistry, *Ab initio* calculations

INTRODUCTION

Metal Schiff base complexes have been investigated because of their interesting and important property such as their ability to reversibly bind oxygen [1]. The applications of these compounds in many areas were increased because of the high stable potential of Schiff base complexes in different oxidation states. They were used as catalysts for oxygenation and oxidation reactions of organic compounds and also electrochemical reduction reactions [2-7]. Vanadyl Schiff bases played a unique role [8] and had been investigated as model compounds to clarify several biochemical processes [9,10]. Also the tridentate vanadyl Schiff base complexes acted as protein tyrosine phosphates inhibitors [11] and showed photo-induced DNA cleavage activities [12].

Thermogravimetry and thermoanalysis techniques are valuable for studying the thermal properties of compounds [13-17]. The electrochemical methods can be envisioned to provide highly valuable information on the catalytic processes since catalytic conversions are frequently accompanied by the change in the oxidation state of the central metal and the structure of the complex. Knowledge of electronic and steric effects to control the redox chemistry of metal Schiff base complexes may prove to be critical in the design of new catalysts. Having continued our studies on vanadyl Schiff base complexes [18-21], herein we report the electronic influence of salicylaldehyde derivatives of ONO tridentate Schiff bases on thermal and electrochemical properties of vanadyl(IV) Schiff base complexes (Fig. 1). The thermal decomposition kinetics parameters, calculate using Coats and Redfern method [22],

*Corresponding author. E-mail: akianfar@cc.iut.ac.ir

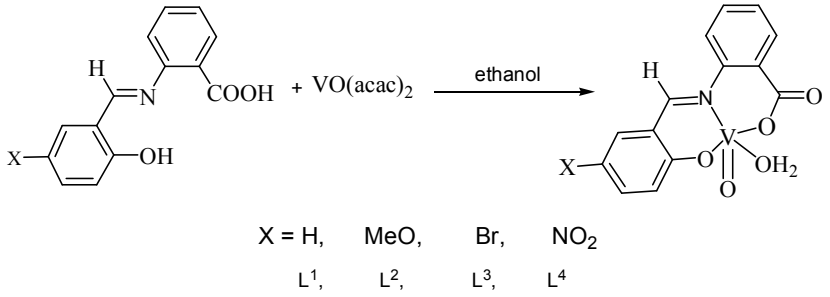

Fig. 1. The structure of vanadyl complexes.

are also reported and discussed. The structures of compounds are determined by *ab initio* calculations. The optimized molecular geometry is calculated at the B3LYP/6-31G(d) level.

EXPERIMENTAL

Chemicals and Apparatus

All of the chemicals and solvents used for synthesis and electrochemistry were of commercially available reagent grade and used without purification. The elemental analysis was done on a CHN-O-Heraeus elemental analyzer. Infrared spectra were recorded as KBr discs on a FT-IR JASCO-680 spectrophotometer in the 4,000-400 cm^{-1}. UV-Vis spectra were recorded on a JASCO V-570 spectrophotometer in the 190-900 nm. Thermogravimetry (TG) and differential thermoanalysis (DTA) were carried out on a PL-1500. The measurements were performed in air atmosphere. The heating rate was kept at 10 °C min^{-1}.

Cyclic voltammograms were performed using an autolab modelar electrochemical system (ECO Chemie, Utr echt, The Netherlands) equipped with a PSTA 20 module and driven by GPES (ECO Chemie) in conjunction with a three-electrode system and a personal computer for data storage and processing. An Ag/AgCl (saturated KCl)/3 M KCl reference electrode, a Pt wire as counter electrode and a glassy carbon electrode as working electrode (Metrohm glassy carbon, 0.0314 cm^2) were employed for the electrochemical studies. Voltammetric measurements were performed at room temperature in dimethylformamide (DMF) solution with 0.1 M tetrabutylammonium perchlorate as the supporting electrolyte.

Synthesis of Schiff Base Ligands

The L^1 Schiff base ligand was synthesized according to the literature [23]. The other tridentate Schiff base ligands, L^2-L^4, were prepared according to the following procedure. The appropriate amounts of salicylaldehyde and its derivatives were added to a methanolic solution of 2-aminobenzoicacid (1:1 mol ratio). The solution was refluxed for 3 h. The precipitate was filtered, washed with methanol and recrystallized by dichloromethane/methanol mixed solvent through the partial evaporation of dichloromethane.

L^1: Yield: 81%, m.p.: 212 °C. IR (KBr pellets, cm^{-1}): 2500-3100 (ν_{OH}), 1685 ($\nu_{C=O}$) and 1617 ($\nu_{C=N}$). λ_{max} (nm) (ε, l mol^{-1} cm^{-1}) (ethanol): 255 (25000), 339 (9800).

L^2: Yield: 82%, m.p.: 190 °C. IR (KBr pellets, cm^{-1}): 2500-3100 (ν_{OH}), 1700 ($\nu_{C=O}$) and 1635 ($\nu_{C=N}$). ^{1}H NMR (DMSO, δH): 12.41 (s, 1H, OH), 10.23 (S, 1H, phenolic, OH), 8.88 (S, 1H, imine), 6.48-7.84 (m, aromatic protons), 3.16-3.73 (m, methoxy), ppm, λ_{max} (nm) (ε, l mol^{-1} cm^{-1}) (Ethanol): 253 (12700), 348 (4900), 430 (1000).

L^3: Yield: 80%, m.p.: 205 °C. IR (KBr pellets, cm^{-1}): 2500-3100 (ν_{OH}), 1700 ($\nu_{C=O}$) and 1636 ($\nu_{C=N}$). λ_{max} (nm) (ε, l $mol^{-1}cm^{-1}$) (ethanol): 257 (10000), 341 (2900), 420 (1100).

L^4: Yield: 76%, m.p.: 273 °C. IR (KBr pellets, cm^{-1}): 2500-3100 (ν_{OH}), 1705 ($\nu_{C=O}$), 1636 ($\nu_{C=N}$) and 1328 (ν_{NO2}). ^{1}H NMR (DMSO, δH): 12.01 (s, 1H, OH), 10.27 (S, 1H, phenolic, OH), 9.08 (S, 1H, imine), 6.45-8.75 (m, aromatic protons), ppm, λ_{max} (nm) (ε, l mol^{-1} cm^{-1}) (ethanol): 277 (8800), 375 (900).

Synthesis of Vanadyl Complexes

The [VOL(OH_2)] complexes were synthesized by adding 1 mmol of Schiff bases to an ethanolic solution of

vanadylacetylacetonate (0.26 g, 1 mmol) and refluxed for 3 h. The reaction mixture was filtered and left to evaporate the ethanol at room temperature. The precipitates were isolated from the solution, washed with ethanol and dried in vacuum.

$[VOL^1(OH_2)]$, (green) Yield: 77%, Anal. Calcd. for $C_{14}H_{11}NO_5V$: C, 51.86; H, 3.40; N, 4.32. Found: C, 51.34; H, 3.52; N, 4.51%. IR (KBr pellets, cm^{-1}): 3363 (ν_{OH}), 1654 ($\nu_{C=O}$), 1606 ($\nu_{C=N}$) and 971 (ν_{VO}), λ_{max} (nm) (ε, l mol^{-1} cm^{-1}) (ethanol): 267 (22000), 340 (sh) 412 (900).

$[VOL^2(OH_2)]$ dark green Yield: 73%, Anal. Calcd. for $C_{15}H_{13}NO_6V$: C, 50.86; H, 3.67; N, 3.95. Found: C, 51.26; H, 3.82; N, 4.21%. IR (KBr pellets, cm^{-1}): 3447 (ν_{OH}), 1639 ($\nu_{C=O}$), 1595 ($\nu_{C=N}$) and 965 (ν_{VO}), λ_{max} (nm) (ε, l mol^{-1} cm^{-1}) (ethanol): 261 (18000), 350 (sh), 430 (1000).

$[VOL^3(OH_2)]$ green Yield: 76%, Anal. Calcd. for $C_{14}H_{10}BrNO_5V$: C, 41.70; H, 2.48; N, 3.47. Found: C, 42.09; H, 2.54; N, 3.61%. IR (KBr pellets, cm^{-1}): 3396 (ν_{OH}), 1596 ($\nu_{C=O}$), 1578 ($\nu_{C=N}$) and 981 (ν_{VO}), λ_{max} (nm) (ε, l mol^{-1} cm^{-1}) (ethanol): 272 (12000), 409 (1600).

$[VOL^4(OH_2)]$ brown Yield: 75%, Anal. Calcd. for $C_{14}H_{10}N_2O_7V$: C, 45.54; H, 2.71; N, 7.58. Found: C, 45.65; H, 2.83; N, 7.72%. IR (KBr pellets, cm^{-1}): 3413 (ν_{OH}), 1606 ($\nu_{C=O}$), 1545 ($\nu_{C=N}$), 1320 (ν_{NO2}) and 911 (ν_{VO}), λ_{max} (nm) (ε, l mol^{-1} cm^{-1}) (ethanol): 277 (7500).

Computational Calculations

Ab initio calculations were carried out using the Gaussian 03 program [24]. The geometries of all the stationary points were optimized at the B3LYP/6-31G(d) level [23]. Harmonic vibrational frequencies were obtained at the B3LYP/6-31G(d) level in order to characterize stationary points as local minima or first-order saddle points. The number of imaginary frequencies (0 or 1) indicates whether a minimum or a transition state was located.

RESULTS AND DISCUSSION

IR Characteristics

The IR spectra of the free Schiff base ligands and the complexes exhibited several bands in the 400-4,000 cm^{-1} region. The OH stretching frequency of the ligands was approved in the range of 2500-3500 cm^{-1} due to the internal hydrogen bonding vibration (O-H…N). This peak is probably overlapped with the acidic OH and the water of KBr. So it was not appeared clearly in the IR spectrum of the ligand. This band disappeared in the spectra of the complexes [16,17,25]. The C=N stretching in the complexes was generally shifted to a lower frequency, indicating a decrease in the C=N bond order due to the coordinate bond formation between the metal and the imine nitrogen lone pair [16,17]. The band at 911-981 cm^{-1} was assigned to V=O stretching. This band was observed as a new peak for the complexes [26].

Electronic Spectra

The spectral data of the free ligands and their complexes are collected in Experimental section. The electronic spectra of the Schiff base ligands and complexes in solution consists of relatively intense bands in the 200-400 nm region, involving internal charge transfer transitions [27]. The L^2 and L^3 Schiff bases show a weak band 400-450 nm related to $n\rightarrow\pi^*$. The bands at about 250-280 nm correspond to $\pi\rightarrow\pi^*$ transitions of aromatic rings in the ligands and complexes.

The Electrochemical Study of Vanadyl Complexes

The cyclic voltammetry of $[VOL(OH_2)]$ complexes were approved out in DMF solution at room temperature. A typical cyclic voltammogram of $[VOL^3(OH_2)]$ complex in the potential range from 0.0-1.0 V (*vs*. Ag/AgCl) was shown in Fig 2. An oxidation peak was observed at about *Ca*. 0.70 V in which $[VOL^3(OH_2)]$ was oxidized to the mono cation $[VOL^3(OH_2)]^+$ in a quasi reversible one-electron step [20].

Numerous scans resulted in virtually superposable cyclic voltammograms, thus showing that the five coordinate geometry is stable in both oxidation states, at least on the cyclic voltammetry time scale. The presence of one peak in the voltammograms revealed that the redox process of all vanadyl Schiff base complexes under study is the one-electron transfer reaction [20]. The oxidation potentials for the different complexes are set out in Table 1. The formal potentials $[E_{1/2}\,(IV \leftrightarrow V)]$ for the V(IV/V) redox couple are calculated as the average of the cathodic (E_{pc}) and anodic (E_{pa}) peak potentials of this process.

To investigation of the effect of functional groups of the

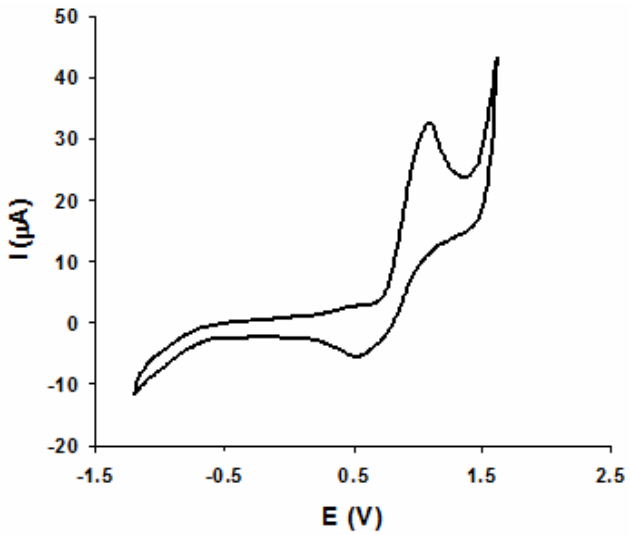

Fig. 2. Cyclic voltammograms of [$VOL^3(OH_2)$], in DMF at room temperature. Scan rate: 100 mV s^{-1}.

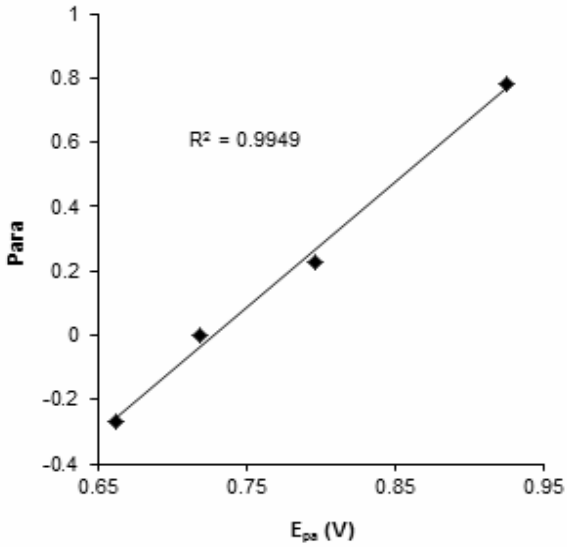

Fig. 3. Correlation between the Epa values for Schiff bases (L^1-L^4) and the respective E_{pa} substituent.

Schiff base ligands on the oxidation potential of [$VOL(OH_2)$], a series of the vanadyl Schiff base complexes were studied by the cyclic voltammetry method. According to the results the anodic peak potential (E_{pa}) varied as it can be expected from the electronic effect of the substituents at position 5. Thus, E_{pa} becomes more positive showed the following trend; MeO < H < Br < NO_2. Similar results have been reported previously for analogous vanadyl(IV), copper(II), nickel(II) and cobalt(III) systems, and have been interpreted by assuming that the strong electron-withdrawing effects stabilized the lower oxidation state while the electro-donating groups had a reverse effect [19-21,28-31]. Hammett-type relationship was found between the E_{pa} values and the appropriate *para* substituent parameters [32], which showed the variation of the electrode potential as a function of the electron withdrawing ability of the substituent at position 5 (Fig. 3) [19-21].

Thermal Analysis

The thermal decomposition of the studied complexes presentes characteristic pathways, depending on the nature of the ligands (Fig. 4). All TG and DTA figures of the other compounds have the same trend. The absence of weight loss up to 80 °C indicates that there is no water molecule in the crystalline solid of studied complexes. Also the TG shows weight loss up to 80 indicating that the water molecule is

Table 1. Redox Potential Data of Vanadyl Complexes in DMF Solution

Compound	E_a	E_c	$E_{1/2}$
$VOL^1(OH_2)$	0.80	0.60	0.70
$VOL^2(OH_2)$	0.55	0.42	0.48
$VOL^3(OH_2)$	0.90	0.60	0.75
$VOL^4(OH_2)$	1.10	0.70	0.90

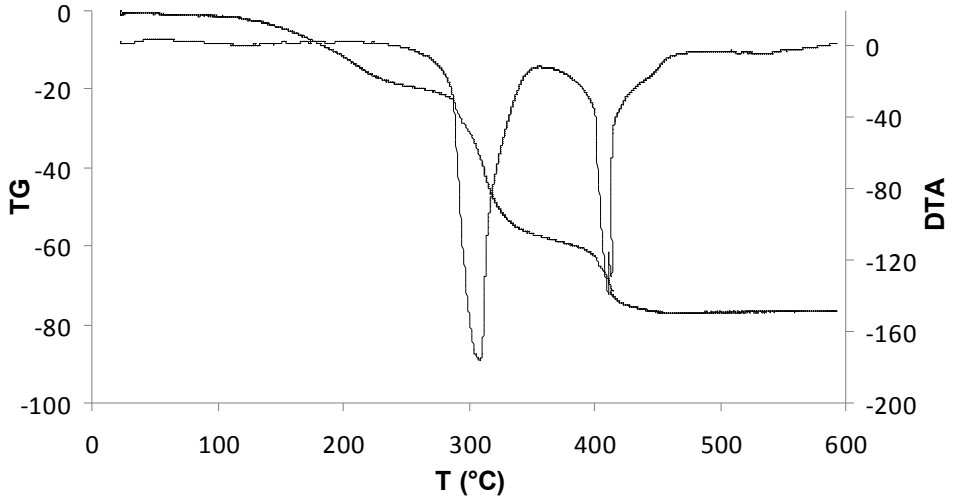

Fig. 4. TG and DTG curve of: $VOL^{2}(OH_2)$.

Table 2. Thermal and Kinetics Parameters for Vanadyl Complexes

Compound	ΔT (°C)[a]	Percent (%)[b]	E* (kJ mol^{-1})	A* (s^{-1})	S* (kJ mol^{-1} K^{-1})	H* (kJ mol^{-1})	G* (kJ mol^{-1})
$VOL^{1}(OH_2)$	35-180	6(5)					
	250-365	45(46)	126.28	1.27×10^{10}	-9.09×10^{1}	123.45	1.54×10^{2}
	366-450	15(16)	101.58	2.33×10^{7}	-1.06×10^{2}	98.26	1.41×10^{2}
$VOL^{2}(OH_2)$	70-244	18(16)					
	244-344	37(34)	79.59	3.47×10^{4}	-1.58×10^{2}	77.07	1.25×10^{2}
	358-452	20(21)	107.84	5.51×10^{7}	-9.94×10^{1}	104.45	1.45×10^{2}
$VOL^{3}(OH_2)$	35-120	9(11)	111.88	6.63×10^{15}	6.88×10^{1}	111.20	1.06×10^{2}
	295-380	18(19)	240.77	2.95×10^{17}	8.79×10^{1}	237.75	2.06×10^{2}
	398-500	37(38)	332.75	1.04×10^{24}	2.11×10^{2}	329.01	2.34×10^{2}
$VOL^{4}(OH_2)$	50-290	3(4)					
	300-380	51(53)	253.17	4.89×10^{18}	-1.12×10^{2}	250.27	2.11×10^{2}
	385-450	16(14)	49.05	7.15×10^{4}	-1.93×10^{2}	45.57	1.26×10^{2}

[a]The temperature range of decomposition pathways. [b]Precent of weight lose found (calculated).

coordinated to the metal center [16,17]. All of the complexes decomposed in three steps (Fig. 4). The temperature range and the percent of loss weight are shown in Table 2.

The [$VOL^1(OH_2)$] complex decomposes in three steps. The first step occurs up to about 125 °C and is attributed to the release of coordinated H_2O. The second step of thermal decomposition occurs in the range of 250-365 °C and is attributed to the release of $C_{12}H_8$. The third mass loss range 366-450 °C is assigned to the rest of the ligand, with the formation of the V_2O_5 [11].

The complex of [$VOL^2(OH_2)$] decomposes in three steps. The step occurs up to about 175 °C is attributed to the release of H_2O and CO functional groups. The second step of thermal decomposition occurs in the range of 244-344 °C, is attributed to the release of C_7H_5N and methoxy functional group. The third mass loss range 358-452 °C is assigned to the rest of the ligand, with the formation of the V_2O_5.

The complex of [$VOL^3(OH_2)$] decomposes in three steps. The step occurs up to about 90 °C is attributed to the release of H_2O and CO. The second step of thermal decomposition occurs in the range of 295-380 °C, is attributed to the release of $C_{12}H_7$.The third mass loss between 398 and 500 °C is assigned to the rest of the ligand, with the formation of the V_2O_5.

The [$VOL^4(OH_2)$] complex decomposes in three steps. The first step occurs up to about 96 °C is relatively attributed to the release of H_2O molecule. The second step of thermal decomposition occurs in the range of 300-380 °C, is attributed to the release of $C_{12}H_7NO_2$. The third mass loss between 385 and 450 °C is assigned to the rest of the ligand, with the formation of the V_2O_5.

Kinetics Aspects

All the well-defined stages were selected to study the kinetics of decomposition of the complexes. The kinetic parameters (the activation energy E and the pre-exponential factor A) were calculated using the Coats–Redfern equation [22],

$$\log\left[\frac{g(\alpha)}{T^2}\right] = \log\frac{AR}{\phi E}\left[1-\frac{2RT}{E_a}\right] - \frac{E_a}{2.303RT}$$

where $g(\alpha) = [(W_f)/(W_f - W)]$, W_f is the mass loss at the end of the reaction, W is the mass loss up to temperature T, R is the gas constant, E_a is the activation energy and Ø is heating rate In the present case, a plot of left hand side (LHS) of this equation against 1/T gives straight line whose slope and intercept are used to calculate the kinetics parameters by the least square method (Fig. 5). The goodness of fit is checked by calculating the correlation coefficient. The other systems and their steps show the same trend.

The entropy of activation $S^{\neq}$was calculated using the equation

$$A = \frac{kT_s}{h}e^{\frac{S^{\neq}}{R}}$$

where k, h and T_s are the Boltzmann constant, the Planck's constant and the peak temperature, respectively. The enthalpy and free energy of activation were calculated using equations

$$E_a = H^{\neq} + RT \quad (3)$$

$$G^{\neq} = H^{\neq} - TS^{\neq} \quad (4)$$

The various kinetic parameters calculated are given in Table 2. The activation energy (E_a) in the different stages are in the range of 49.05-332.75 kJ mol^{-1}. The respective values of the pre-exponential factor (A) vary from 3.47 × 10^4 to 1.04 × 10^{24} s^{-1}. The corresponding values of the entropy of activation ($S^{\neq}$), the enthalpy of activation ($H^{\neq}$) and the free energy of activation ($G^{\neq}$) are in the range of -1.93 × 10^2-2.11 × 10^2 kJ mol^{-1}, 45.57-329.01 kJ mol^{-1} and1.06 × 10^2-2.34 × 10^2 kJ mol^{-1}, respectively. There is no definite trend in the values of activation parameters among the different stages in the present series. The negative values of entropy of activation indicate that the activated complex has a more ordered structure than the reactants [33,34].

Molecular Structure and Analysis of Bonding Modes

The structures of the ligands and the geometry around of vanadyl atom in the complexes were determined by *ab initio* calculations. Also the bond lengths and angles were studied

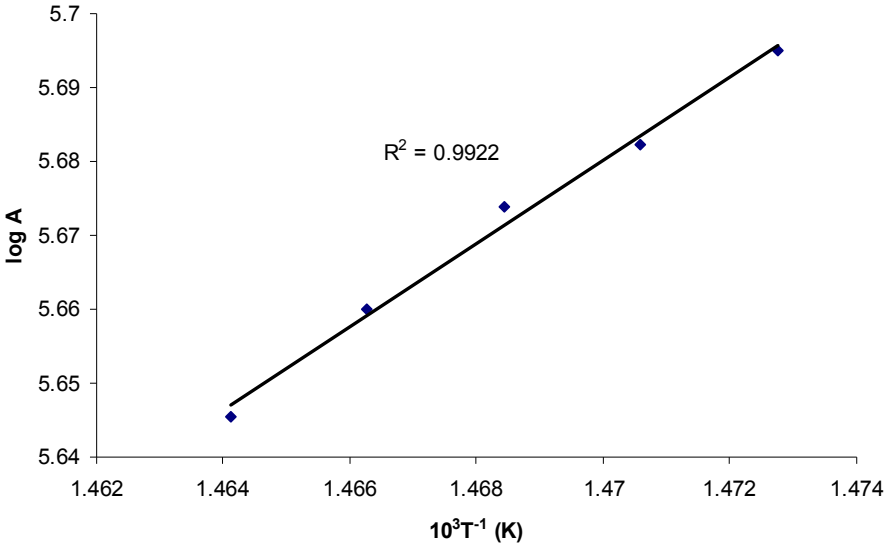

Fig. 5. Coats-Redfern plots of $[VOL^2(OH_2)]$ complex, step 3, $A = \dfrac{\log \dfrac{W_f}{W_f - W}}{T^2}$

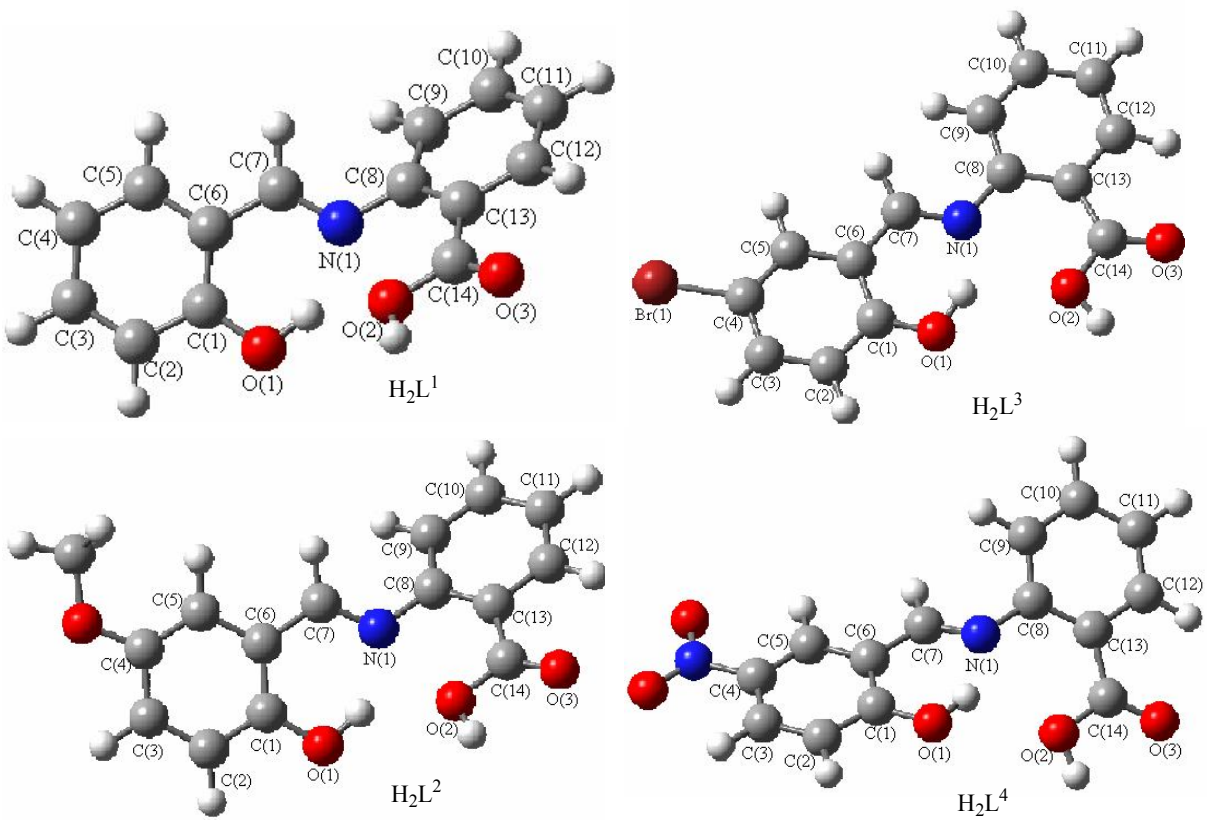

Fig. 6. Optimized structures of Schiff base ligands.

and compared. The geometries of the Schiff base ligands and complexes were represented in Fig. 6. Significant bond lengths and bond angles were also reported in Table 3. According to the theoretical studies, the Schiff base ligands had neutral structure. The C-N bond lengths were increased according to the trend of C(7)-N(1) < C(8)-N(1). This was due to the double and single bond character of C(7)-N(1) and C(8)-N(1), respectively.

The geometries of the complexes are represented in Fig. 7. Significant bond lengths and bond angles are also reported in Table 4. The total energies, zero point energies and dipole moments of the ligands and the complexes are also presented in Table 5.

It was shown that for the L^1, L^2 and L^4 complexes, V(IV) ion is in square-pyramid NO_4 coordination geometry while in $VOL^3(OH_2)$ complex V(IV) ion is in TBP (trigonal bipyramidal) NO_4 coordination geometry similar to that reported for vanadium complexes [35-37]. The bond angle of O(2)-V(1)-O(3) was smaller than O(1)-V(1)-N(1), O(2)-V(1)-N(1) and O(1)-V(1)-O(3) because of intermolecular hydrogen bonds between the acid group oxygen with the hydrogen of the H_2O molecule. All distances and angles in the studied complexes agreed well with the same distances and angles reported for the other vanadyl complexes. For example the V(1)-O(4) bond distance was found in the range of 1.53-1.62 A˚ (Table 4) that was in good agreement with the value that reported previously [35,36].

CONCLUSIONS

Taking into consideration the electrochemical and thermogravimmetrical properties of vanadyl tridentate

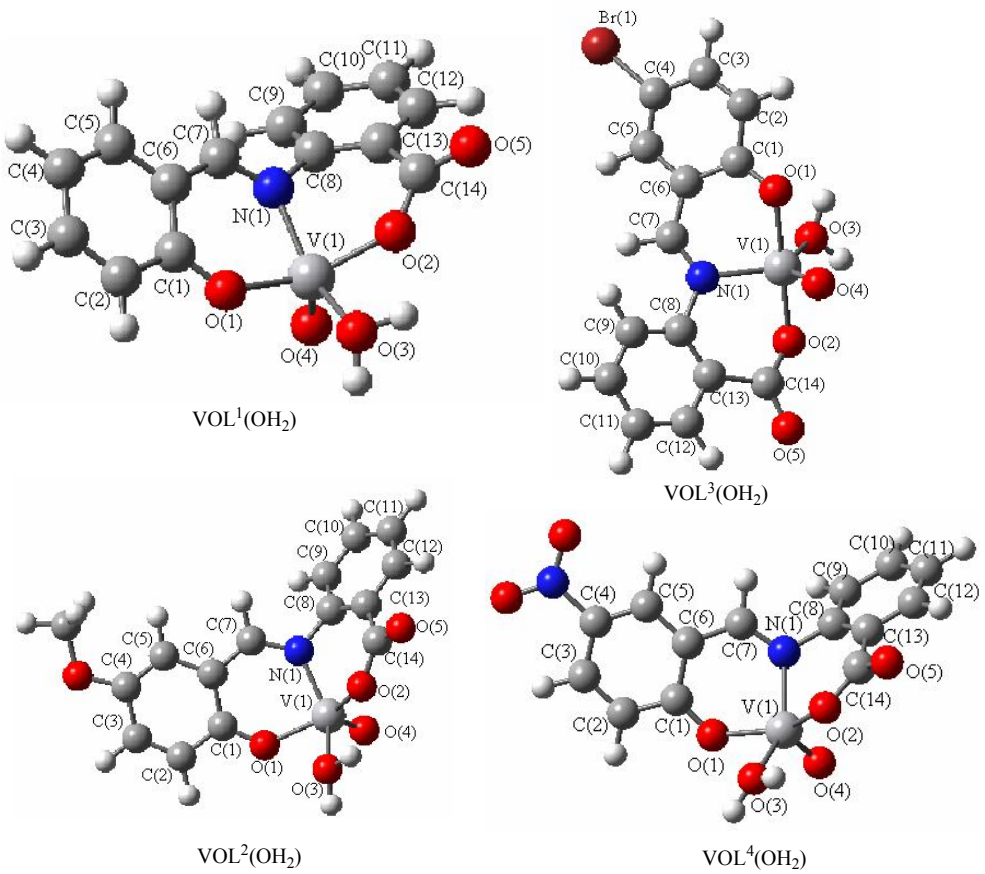

$VOL^1(OH_2)$ $VOL^3(OH_2)$

$VOL^2(OH_2)$ $VOL^4(OH_2)$

Fig. 7. Optimized structures of complexes.

Table 3. Signeficent Bond Lenghts and Bond Angles Calculated at the B3LYP/6-31G(d) Level

Structural parameter	H_2L^1	H_2L^2	H_2L^3	H_2L^4
Bond lenghts (Å)				
O(1)-C(1)	1.34	1.34	1.33	1.33
C(6)-C(7)	1.45	1.45	1.44	1.45
C(7)-N(1)	1.29	1.29	1.29	1.29
C(8)-N(1)	1.40	1.39	1.39	1.40
C(13)-C(14)	1.49	1.49	1.49	1.49
C(14)-O(2)	1.35	1.35	1.35	1.35
C(14)-O(3)	1.22	1.22	1.21	1.21
Bond angles (°)				
O(1)-C(1)-C(2)	118.20	118.16	118.04	118.14
O(1)-C(1)-C(6)	122.59	123.09	122.79	122.40
C(1)-C(6)-C(7)	121.44	121.29	122.25	121.36
C(5)-C(6)-C(7)	119.61	119.03	118.79	119.55
C(6)-C(7)-N(1)	122.22	122.26	122.58	121.52
C(7)-N(1)-C(8)	121.29	121.29	122.59	121.47
C(9)-C(8)-N(1)	120.32	120.41	122.15	120.29
C(13)-C(8)-N(1)	121.13	121.11	120.13	120.93
C(8)-C(13)-C(14)	126.09	126.09	128.86	126.18
C(12)-C(13)-C(14)	114.84	114.82	112.30	114.86
C(13)-C(14)-O(3)	123.43	115.58	123.27	123.42
O(2)-C(14)-O(3)	120.99	120.99	120.15	121.04
O(2)-C(14)-C(13)	115.57	115.58	116.46	115.54

Schiff base complexes and *ab initio* calculations the following conclusions have been made.

The cyclic voltammetry of the complexes shows that the anodic peak potentials E_{pa} of different substituent increase *via* increasing the electron withdrawing property of the Schiff base. According to the thermogravimetry results the thermal decomposition pathways of the complexes are related to the Schiff base properties and also are first order in all steps for the studied complexes. The theoretical studies show that the geometry of the complexes around the vanadyl atom is square-pyramide and trigonal bipyramidal NO_4.

Table 4. Signeficent Bond Lenghts and Bond Angles Calculated at the B3LYP Method with 6-31G(d) Basis Set

Structural parameter	$VOL^1(OH_2)$	$VOL^2(OH_2)$	$VOL^3(OH_2)$	$VOL^4(OH_2)$
Bond lenghts (Å)				
O(1)-C(1)	1.27	1.27	1.27	1.28
O(2)-C(14)	1.33	1.33	1.30	1.33
N(1)-V(1)	2.01	1.99	2.00	2.02
O(1)-V(1)	1.98	1.99	2.07	1.98
O(2)-V(1)	1.92	1.92	1.98	1.92
O(3)-V(1)	2.11	2.09	2.11	2.07
O(4)-V(1)	1.54	1.54	1.62	1.53
Bond angles (°)				
O(1)-V(1)-N(1)	87.11	86.99	89.47	86.69
O(2)-V(1)-N(1)	87.56	88.22	90.57	87.08
O(1)-V(1)-O(3)	85.93	84.73	91.84	86.11
O(2)-V(1)-O(3)	75.94	74.86	88.14	78.84
O(4)-V(1)-N(1)	107.59	110.46	115.03	109.72
O(4)-V(1)-O(1)	107.75	104.92	88.51	103.75
O(4)-V(1)-O(2)	114.46	111.46	91.48	108.54
O(4)-V(1)-O(3)	105.40	110.72	126.41	109.27

Table 5. Total Energies (Corrected with Zero Point Energies), (with Zero Point Energy Correction) E (Hartree), Zero Point Energys ZPE ($kJ\ mol^{-1}$) and Dipole Moments μ (D) of the Isomers of Ligands Calculated at the B3LYP Level Using a 6-31G(d) Basis Set

Compound	E	ZPE	μ
H_2L^1	-820.327592	585.2	3.37
H_2L^2	-934.814595	671.0	4.28
H_2L^3	-3391.434024	558.4	2.02
H_2L^4	-1024.828494	592.2	3.82

REFERENCES

[1] S. Park, V.K. Mathur, R.P. Planap, Polyhedron 17 (1998) 325.

[2] A. Nashinaga, H. Ohara, H. Tomita, T. Matsuura, Tetrahedron Lett. 24 (1983) 213.

[3] L. Canali, D.C. Sherrigton, Chem. Soc. Rev. 28 (1998) 85.

[4] A.A. Isse, A. Gennaro, E. Vianello, J. Electroanal. Chem. 444 (1998) 241.

[5] D. Pletcher, H. Thompson, J. Electroanal. Chem. 464 (1999) 168.

[6] T. Okada, K. Katou, T. Hirose, M. Yuasa, I. Sekine, J. Electrochem. Soc. 146 (1999) 2562.

[7] H. Aghabozorg, N. Firoozi, L. Roshan, H. Eshtiagh-Hosseini, A.R. Salimi, M. Mirzaei, M. Ghanbari, M. Shamsipur, M. Ghadermazi, J. Iran. Chem. Soc. 8 (2011) 992.

[8] V. Conte, B. Floris, Inorg. Chem. Acta 363 (2010) 1935.

[9] D. Rehder, Angew. Chem. Int. Ed. Engl. 30 (1991) 148.

[10] A. Butler, C.J. Carrano, Coord. Chem. Rev. 109 (1991) 61.

[11] C. Yuan, L. Lu, Y. Wu, Z. Liu, M. Guo, S. Xing, X. Fu, M.J. Zhu, Inorg. Biochem. 104 (2010) 978

[12] P. Prasad, P.K. Sasmal, I. Khan, P. Kondaiah, A.R. Chakravarty, Inorg. Chem. Acta (in press).

[13] E.A. Pedro, M.S. Joa˜o, R. Sandra, A.R. Luiz, P.S. Mirian, R.D. Edward, T.G.C. Eder, Thermochim. Acta 453 (2007) 9.

[14] A.A. Soliman, W. Linert, Thermochim. Acta 338 (1999) 67.

[15] A.A. Soliman, J. Thermal. Anal. Calorim. 63 (2001) 221.

[16] B.S. Garg, D.N. Kumar, Spectrochimica Acta Part A 59 (2003) 229.

[17] A. Anthonysamy, S. Balasubramanian, Inorg. Chem. Commun. 8 (2005) 908.

[18] A.H. Kianfar, S. Mohebbi, J. Iran. Chem. Soc. 4 (2007) 215.

[19] A.H. Kianfar, V. Sobhani, M. Dostani, M. Shamsipur, M. Roushani, Inorg. Chem. Acta 355 (2011) 108.

[20] A.H. Kianfar, M. Paliz, M. Roushani, M. Shamsipour, Spectrochimica Acta Part A 82 (2011) 44.

[21] A.H. Kianfar, S. Asle Khademi, R. Hashemi Fath, M. Roushani, M. Shamsipur, J. Iranian. Chem. Soc. 2013, impress.

[22] A.W. Coats, J.P. Redfern, Nature 201 (1964) 68.

[23] R. Johari, G. Kumar, D. Kumar, S. Singh, J. Indian Council of Chemists 26 (2009) 23.

[24] M.J. Frisch, G.W. Trucks, H.B. Schlegel, G.E. Scuseria, M.A. Robb, J.R. Cheeseman, J.A. Montgomery, J.T. Vreven, K.N. Kudin, J.C. Burant, J.M. Millam, S.S. Iyengar, J. Tomasi, V. Barone, B. Mennucci, M. Cossi, G. Scalmani, N. Rega, G.A. Petersson, H. Nakatsuji, M. Hada, M. Ehara, K. Toyota, R. Fukuda, J. Hasegawa, M. Ishida, T. Nakajima, Y. Honda, O. Kitao, H. Nakai, M. Klene, X. Li, J.E. Knox, H.P. Hratchian, J.B. Cross, C. Adamo, J. Jaramillo, R. Gomperts, R.E. Stratmann, O. Yazyev, A.J. Austin, R. Cammi, C. Pomelli, J.W. Ochterski, P.Y. Ayala, K. Morokuma, G.A. Voth, P. Salvador, J.J. Dannenberg, V.G. Zakrzewski, S. Dapprich, A.D. Daniels, M.C. Strain, O. Farkas, D.K. Malick, A.D. Rabuck, K. Raghavachari, J.B. Foresman, J.V. Ortiz, Q. Cui, A.G. Baboul, S. Clifford, J. Cio-slowski, B.B. Stefanov, G. Liu, A. Liashenko, P. Piskorz, I. Komaromi, R.L. Martin, D.J. Fox, T. Keith, M.A. Al-Laham, C.Y. Peng, A. Nanayakkara, M. Challacombe, P.M.W. Gill, B. Johnson, W. Chen, M.W. Wong and C. Gonzalez, A. Pople, 2003 Gaussian 03: Revision B.05. Gaussian, Pittsburgh.

[25] D.N. Kumar, B.S. Garg, Spectrochimica Acta Part A 59 (2006) 141.

[26] M. Mathew, A.J. Gary, G.J. Palenik, J. Am. Chem. Soc. 92 (1972) 3197.

[27] A.H. Kianfar, L. Keramat, M. Dostani, M. Shamsipur, M. Roshani, F. Nikpour, Spectrochemica Acta 77 (2010) 424.

[28] A.H. Sarvestani, A. Salimi, S. Mohebbi, R. Hallaj, J. Chem. Res. (2005) 190.

[29] A.H. Sarvestani, S. Mohebbi, J. Chem. Res. (2006) 257.

[30] E.G. Ja¨ger, K. Schuhmann, H. Go¨rls, Inorg. Chem. Acta 255 (1997) 295.

[31] S. Zolezzi, E. Spodine, A. Decinti, Polyhedron 21

(2002) 55.
[32] H.H. Jaffe, Chem. Rev. 53 (1953) 191.
[33] S. Mathew, C.G.R. Nair, K.N. Ninan, Thermochim Acta 155 (1989) 247.
[34] M.K.M. Nair, P.K. Radhakrishnan, Thermochim Acta 261 (1995) 141.
[35] C. Cordelle, D. Agustin, C.D. Jean, R. Poli, Inorg. Chim. Acta 364 (2010) 144.
[36] M. Ebel, D. Rehder, Inorg. Chim. Acta 356 (2003) 210.
[37] E.B. Seena, N. Mathew, M. Kuriakose, M.R. Prathapachandra Kurup, Polyhedron 27(2008) 1455.